



Thermodynamic Analysis of a Combined Single Effect Vapour Absorption System and tc-CO₂ Compression Refrigeration System

Abhishek Verma ^a, S. C. Kaushik ^a , S. K. Tyagi ^{a*} 

^a Centre for Energy Studies, Indian Institute of Technology Delhi, Hauz Khas, New Delhi-110016, India.

Received 22 September 2020; Revised 14 March 2021; Accepted 16 April 2021; Published 01 June 2021

Abstract

The transcritical CO₂ refrigeration system is coupled with the single effect vapour absorption with LiBr-water as a working pair, having the objective of enhancing the performance of the low temperature transcritical refrigeration system while using a natural working pair and reducing the electricity consumption to produce low temperature refrigeration. The high grade waste heat rejected in the gas cooler of the tc-CO₂ compression refrigeration system (TCRS) is utilized to run the single effect vapour absorption system (SEVAR) to enhance the energy efficiency of the system. The gas cooler in the transcritical CO₂ system has heat energy at a high temperature and pressure, which is utilized to run the vapour absorption system, while the other refrigerant heat exchanger provides subcooling to further enhance the performance. The combined cycle can provide refrigeration temperature at different levels, to use it for different applications. Energetic and exergetic analysis have been done to analyze the combined system to compute the performance parameters and the irreversibilities occurring in different components to further increase the performance. The combined system is optimized for various heat rejection and refrigeration temperatures. The COP of the combined system has been enhanced by 24.88% while the enhancement in exergetic efficiency (η_{ex}) is observed at 10.14%, respectively, over tradition transcritical CO₂ compression refrigeration system, with -10°C as an evaporation (TCRS cooling) temperature and the exit temperature of gas cooler T₄ being 40°C.

Keywords: Exergy; Vapour Absorption; Carbon Dioxide; Waste Heat; Transcritical.

1. Introduction

Refrigeration and air conditioning play a vital role in almost every sector of society. Global warming and the depletion of the ozone layer have become the key issues for conventional refrigeration systems. In 1987, the Montreal Protocol [1] set a time limit for the usage of chlorofluorocarbon (CFC) and hydrochlorofluorocarbon (HCFC) refrigerants, as they are responsible for ozone depletion, but the use of hydrofluorocarbons (HFC)s was being the major concern as its effects are hazardous for the environment and climate change. In 1997, the Kyoto Protocol [2] limited the use of HFCs with large GWP. In 1998, Robinson and Groll [3] suggested the use of naturally occurring refrigerants, which do have a low GWP and environment friendly. CO₂ as a naturally occurring refrigerant having good thermophysical properties [4] finds favour across almost all sectors of refrigeration to be used as the refrigerant [5]. It has a critical temperature of 30.85°C [3]. Transcritical CO₂ (R744) has been adopted worldwide for supermarkets, food storage, industrial applications, etc., even in locations having high ambient temperatures [6]. In CO₂ refrigeration systems, subcooling plays an important role in upgrading the performance of the system. Dedicated subcooling methods improve COP by 30%, thermoelectric systems by 25.6%, internal heat exchangers improve COP by 12 while 22% with economizers [7]. In a CO₂ refrigeration system, Bellos and Tzivanidis [8] reported that the performance of the system upto 75% by the use of a mechanical subcooling system over the basic configuration. Use

* Corresponding author: tyagisk@ces.iitd.ac.in; sudhirtyagi@yahoo.com

 <http://dx.doi.org/10.28991/HIJ-2021-02-02-02>

➤ This is an open access article under the CC-BY license (<https://creativecommons.org/licenses/by/4.0/>).

© Authors retain all copyrights.

of ejector and thermoelectric subcooling enhance the performance upto 40% [9]. Internal heat exchangers for subcooling improve the COP by 12 and 25% by using thermoelectric subcooling for specific operating conditions [10].

Mohammadi [11] studied various configurations of the CO₂ refrigeration system coupled with different absorption chillers to produce refrigeration at different temperature levels from -80°C to -30°C with an increase of COP upto 200% in a few cases. The mean COP improvement for CO₂ refrigeration systems has been reported to be 23% with subcooling by absorption chillers [12]. The net impact of GWP is 1 for CO₂ refrigeration systems [13]. Basso et al. [14] integrated the transcritical CO₂ heat pump to reduce the load of the external heat source for a hybrid system using dynamic simulation. The working pair used in the absorption refrigeration system is ecofriendly, non-flammable, and non-toxic in nature, having low operating pressures [15]. Presently, the emphasis is on energy-efficient systems to fulfill the demand for refrigeration and air conditioning (RAC) in society. To improve the energy efficiency of the system, exergy analysis is the preferred tool to be used as it is defined as the potential of a stream to cause change, as well as it tells the quality of the system as an effective portion of the potential of the system to have an impact on the environment [16, 17]. It also quantifies the irreversibilities occurring in components of the system.

The reported literature review suggests that subcooling the tc-CO₂ system has been showing promising enhancement in the performance of the system. Thus, coupling the absorption system with the tc-CO₂ system improves the overall system performance and provides refrigeration with different temperature levels. The present study focuses on the use of waste heat to run the single effect vapour absorption system (SEVAR). The waste heat being rejected in the gas cooler (GC) of the tc-CO₂ compression refrigeration system (TCRS) [18] is being utilized to run SEVARs, which improves the energy efficiency of the combined system. The exergy analysis and parametric study of the combined system are being presented.

2. System Description

The SEVARs are coupled with TCRS. The superheated refrigerant (CO₂) is compressed in a compact compressor to a high temperature and pressure. The heat rejection of high pressure and temperature CO₂ that occurred in gas cooler 1 (GC1) and gas cooler 2 (GC₂) is utilized by circulating the water. In GC1, water at 1 atmospheric pressure and 100°C enters and changes its phase from liquid water to saturated steam at constant temperature of 100°C, as the temperature of CO₂ is well above 100°C. The generated saturated steam is utilized as the heat input to the SEVARs, where the generator is kept at 90°C [10]. The temperature of the refrigerant (CO₂) is still higher (more than 100°C) after rejecting heat in GC₁, so it is required to further reject heat in GC₂ to an optimum gas cooler temperature of 40°C, by circulating the water at 25°C at 1 atm pressure. The hot water obtained from GC₂ can be utilized for various applications, such as desalination, distillation, industrial and domestic uses [17].

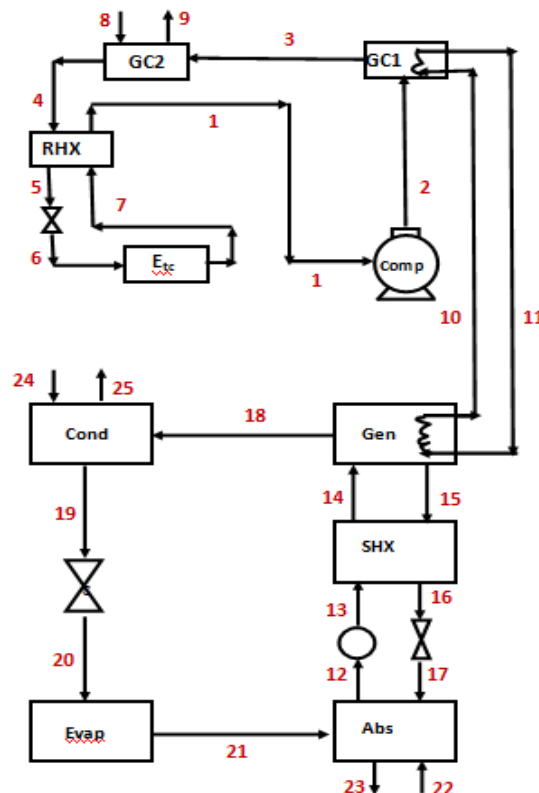


Figure 1. TCRS coupled with SEVARs

Further the refrigerant is passed through refrigerant heat exchanger (RHX_{TC}), to improve the efficiency of TCRS and expanded through the refrigerant throttling valve RTV_{TC}. The refrigerant CO₂ is expanded upto a low temperature of -10°C. The saturated refrigerant vapour at the exodus of evaporator gets superheated vapour while exchanging heat in RHX_{TC} which reduces the compressor work considerably. The working of SEVAR Libr-H₂O based system has reported by various authors [19-23].

3. Thermodynamic Analysis

3.1. System Model

The analysis of the combined cycle includes mass balance, concentration balance, energy balance and exergy balance for individual component and is presented as [16, 22]:

$$\sum \dot{m}_i - \sum \dot{m}_e = 0 \quad (1)$$

$$\sum \dot{m}_i \dot{x}_i - \sum \dot{m}_e \dot{x}_e = 0 \quad (2)$$

$$\sum \dot{Q} - \sum \dot{W} = \sum \dot{m}_e \dot{h}_e - \sum \dot{m}_i \dot{h}_i \quad (3)$$

Form 1st law of thermodynamics (FLT), the (COP) of TCRS is given as:

$$COP_{TC} = \frac{\dot{Q}_{Etc.}}{\dot{W}_C} \quad (4)$$

Form 1st law of thermodynamics (FLT), the (COP) of VARS is given as:

$$COP_{VA} = \frac{\dot{Q}_{Eva.}}{\dot{Q}_G + \dot{W}_P} \quad (5)$$

Form 1st law of thermodynamics (FLT), the (COP) of combined is given as:

$$COP_{NET} = \frac{\dot{Q}_{Etc.} + \dot{Q}_{Eva.}}{\dot{W}_C} \quad (6)$$

Exergy flow rate for a stream on each state is defined as:

$$\dot{E} = \dot{m}[(h - h_0) - T_0(s - s_0)] \quad (7)$$

Considering a steady state process, the exergy destruction rate ($\dot{E}D$) to a component is specified as [16, 24]:

$$\dot{E}D = \sum \dot{E}_i - \sum \dot{E}_e + \sum \dot{Q} \left(1 - \frac{T_0}{T}\right) - \sum \dot{W} \quad (8)$$

Based on 2nd law of thermodynamics (SLT), the performance parameter (exergetic efficiency) for the system given as [16, 24]:

$$\eta_{exTC} = \frac{\dot{Q}_{Etc.} \left|1 - \frac{T_0}{T_{r_{tc}}}\right|}{\dot{W}_C} \quad (9)$$

$$\eta_{exVA} = \frac{\dot{Q}_{Eva.} \left|1 - \frac{T_0}{T_{r_{va}}}\right|}{\dot{Q}_G \left|1 - \frac{T_0}{T_G}\right| + \dot{W}_P} \quad (10)$$

$$\eta_{exNET} = \frac{\left(\dot{Q}_{Etc.} \left|1 - \frac{T_0}{T_{r_{tc}}}\right| + \dot{Q}_{Eva.} \left|1 - \frac{T_0}{T_{r_{va}}}\right|\right)}{\dot{W}_C + \dot{W}_P} \quad (11)$$

3.2. Assumptions

The following have been made to analyze the combined system:

- Entirely, individual components of the combined system are considered as control volume.
- The combined system follows steady state conditions.
- The pressure drop in connecting lines and components is neglected.

- The temperature of the refrigerated space required is supposed to be 5°C higher to the respective evaporator temperature.
- The refrigerant (water) leaving condenser of SEVAR is considered to be saturated liquid.
- The exodus of evaporator is considered to be saturated vapour.
- Pumping in SEVAR is considered to be isentropic [19].
- Entropy change through the solution throttling valve (STV) is derelicted and the temperature is expected to be constant [19].
- The SEVARs is well away from crystallization.
- Water at 25°C, 1 atm is used to cool the GC₂ TCRS and condenser & absorber of SEVARs.

3.3. Research Methodology

The research methodology has been explained in the flowchart for the combined analysis of the coupled cycle.

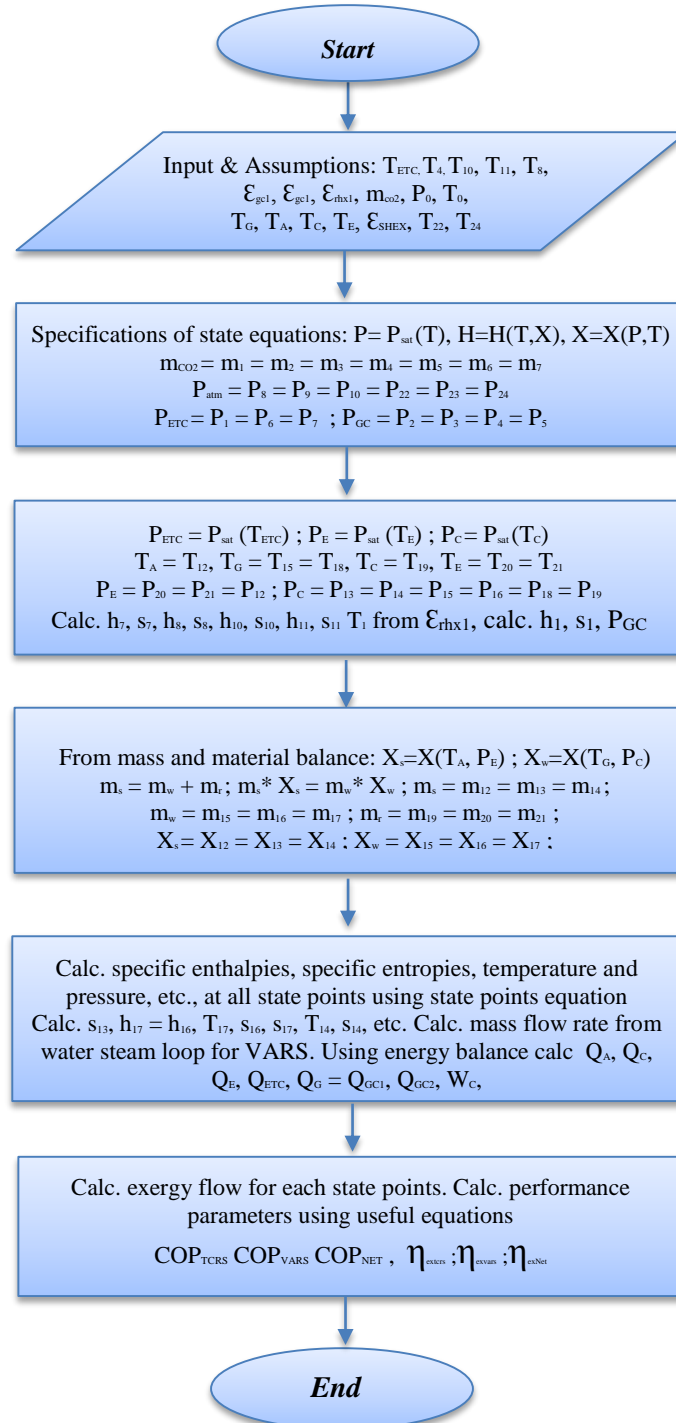


Figure 2. Flowchart for the analysis of the combined cycle

3.4. Input parameters

- Isentropic efficiency of compressor is [3]:

$$\eta_c = 0.815 + 0.022r_p - 0.0041(r_p)^2 + 0.0001(r_p)^3 \tag{12}$$

- Generator temperature, (T_g) = 90°C;
- Evaporator temperature in SEVARS, T_{eva} = 7°C;
- Mass flow rate of refrigerant (CO₂) in TCRS, m_{trc} = 1 kg/s;
- Effectiveness of gas cooler 1, (ε_{gc1})= 0.8;
- Effectiveness of gas cooler 2, (ε_{gc2})= 0.8;
- Effectiveness of solution heat exchanger (SHX), ε_{shx} = 0.7;
- Condenser and absorber temperatures, T_{cond} = T_a = 35°C.

4. Results and Discussion

4.1. Simulation Validation

The validation of the combined system, has been done by validating the two cycles separately as there is no literature available for this coupled cycle in this manner. The analysis of single effect VARS cycle is compared with the results presented by Kaushik and Arora [20]. The input parameters considered for the validation of cycle are: T_E=7.2°C, T_G=87.8°C, T_A = T_C = 37.8 °C, solution heat exchanger effectiveness = 0.7, refrigerant mass flow rate = 1 kg/s. Table. Shows the comparison of the results obtained by the Kaushik and Arora [20] and the present study for energy transfer involved in various components and the COP of the system. It is seen that the there is a good agreement among the results obtained in the present study and those available in the literature. Also, Figures 3 and 4 show that the variation of COP with generator temperature ant various absorber temperature shows similar trends for the present study and those reported in the literature. Thus, the present validation of the system is reliable.

Table 1. Energy analysis comparison of present work with numerical values given in Kaushik & Arora [20] for SEVARS

Input Data : T _E =7.2°C, T _G =87.8°C, T _A = T _C = 37.8 °C, solution heat exchanger effectiveness = 0.7, refrigerant mass flow rate = 1 kg/s				
S. No.	Component	Kaushik & Arora [20]	Present study	Difference
		Q (kW)	Q (kW)	(%)
1.	Generator	3095.7	3096	-0.00969
2.	Absorber	2945.27	2946	-0.02479
3.	Condenser	2505.91	2506	-0.00359
4.	Evaporator	2355.45	2355	0.019105
5.	Solution Heat Exchanger	518.72	519.5	-0.15037
6.	Solution throttle valve	0	0	-
7.	Refrigerant throttle valve	0	0	-
8.	Pump	0.0314	0.03093	1.496815
9.	Energy Input	5451	5451	0
10.	COP (No Dimensions)	0.7609	0.7608	-

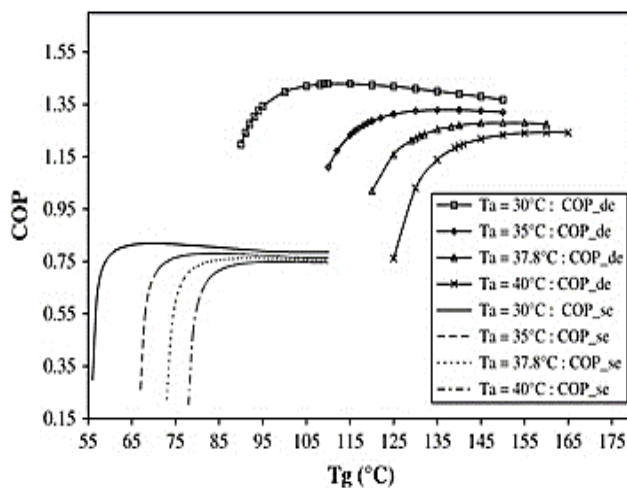


Figure 3. COP variation with generator temperature in single effect systems, (Kaushik and Arora [20])

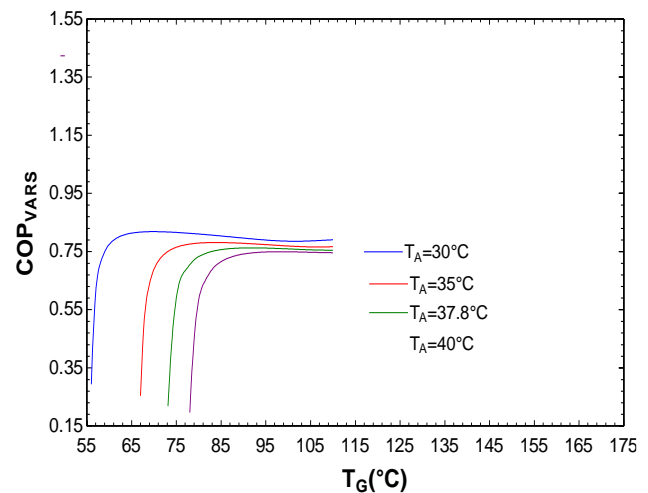


Figure 4. COP variation with generator temperature in single effect systems (Present study)

4.2. COP and Exergetic Efficiency

The trend of COP with gas cooler pressure P_{GC} and exergetic efficiency (η_{ex}) with P_{GC} is shown in Figure 5, having GC_2 outlet temperature to be $40^\circ C$. The COP and exergetic efficiency (η_{ex}) of the system increases as the P_{GC} increases upto an optimum gas cooler pressure and then started decreasing gradually. At constant gas cooler outlet temperature, the P_{GC} increases the refrigerating capacity and the compressor work, while initially the rate of increase in refrigerating effect is more hence the exergetic efficiency (η_{ex}) and COP and increases upto an optimum P_{GC} and further decreases gradually beyond this optimum P_{GC} as shown in Table 2. For an evaporation (cooling) temperature of $-10^\circ C$, in TCRS, outlet temperature of gas cooler T_4 being $40^\circ C$, the optimum P_{GC} is found to be approx. 10 MPa. The thermodynamic state points, energy transfer, exergy destruction are computed in Tables 5-7. The performance parameters of the combined system is compared with the base case of TCRS and accessible in Table 6.

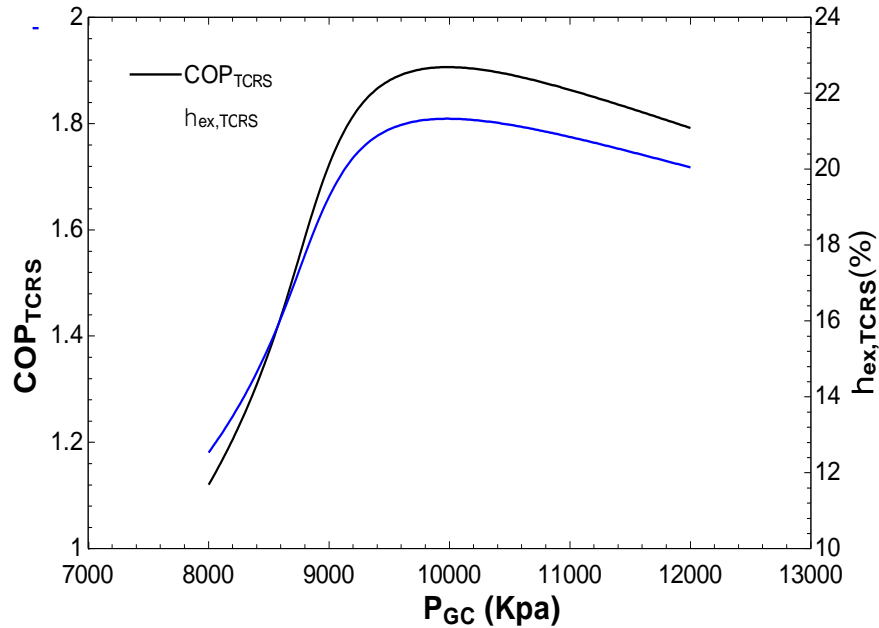


Figure 5. Influence of P_{GC} on COP and η_{ex} of TCRS

Table 2. The deviation of power input (W), refrigerating effect (Q_{Etc}), COP & exergetic efficiency (η_{ex}) of TCRS with pressure of gas cooler for ($T_4= 40^\circ C$) and ($T_{Etc} = -10^\circ C$)

P_{GC} (MPa)	W (kW)	Q _{Etc} (kW)	COP _{TCRS}	$\eta_{ex,TCRS}$
8.0	72.72	81.46	1.12	12.53
8.2	74.56	89.89	1.206	13.49
8.4	76.36	99.97	1.309	14.65
8.6	78.14	112.2	1.436	16.07
8.8	79.89	126.7	1.586	17.74
9.0	81.61	140.6	1.723	19.27
9.2	83.3	151.1	1.814	20.3
9.4	84.98	158.5	1.866	20.87
9.6	86.63	163.9	1.892	21.17
9.8	88.26	168	1.903	21.3
10.0	89.87	171.3	1.906	21.33
10.2	91.46	174.1	1.903	21.29
10.4	93.04	176.4	1.896	21.22
10.6	94.59	178.5	1.887	21.11
10.8	96.14	180.3	1.876	20.99
11.0	97.66	182	1.863	20.85
11.2	99.18	183.5	1.85	20.7
11.4	100.7	184.8	1.836	20.54
11.6	102.2	186.1	1.821	20.38
11.8	103.6	187.2	1.807	20.21
12.0	105.1	188.3	1.792	20.04

Table 3. State points obtained by thermodynamic analysis

State	T (°C)	s (kJ/kgK)	h (kJ/kg)	x	m (kg/s)	P (kPa)
1.	30	-0.6658	-22.42	-	1	2649
2.	151.9	-0.6325	67.48	-	1	10004
3.	110.4	-0.7685	12.61	-	1	10004
4.	40	-1.383	-193.8	-	1	10004
5.	27.51	-1.543	-243	-	1	10004
6.	-10	-1.492	-243	-	1	2649
7.	-10	-0.8405	-71.64	-	1	2649
8.	25	0.3669	104.8	-	0.7217	101.3
9.	93.3	1.231	390.8	-	0.7217	101.3
10.	100	1.307	419.1	-	0.02432	101.3
11.	100	7.354	2676	-	0.02432	101.3
12.	35	0.2184	81.15	0.5408	0.1091	1.002
13.	35	0.2184	81.16	0.5408	0.1091	5.627
14.	62.29	0.3945	137.7	0.5408	0.1091	5.627
15.	90	0.4751	239.6	0.6477	0.09108	5.627
16.	51.93	0.2775	171.9	0.6477	0.09108	5.627
17.	51.93	0.2775	171.9	0.6477	0.09108	1.002
18.	90	8.662	2669	0	0.01802	5.627
19.	35	0.505	146.6	0	0.01802	5.627
20.	7	0.5246	146.6	0	0.01802	1.002
21.	7	8.973	2513	0	0.01802	1.002
22.	25	0.3669	104.8	-	1	101.3
23.	37.45	0.5381	156.9	-	1	101.3
24.	25	0.3669	104.8	-	1	101.3
25.	35.86	0.5166	150.3	-	1	101.3

Table 4. Energy transfer in various components

Component	Q (kW)	W (kW)
TCRS		
Evaporator	171.4	-
Compressor	-	134.7
Gas Cooler (GC ₁)	54.87	-
Gas Cooler (GC ₂)	206.4	-
RHX	54.9	-
VARS		
Evaporator	42.64	-
Condenser	45.43	-
Absorber	52.08	-
Generator	54.87	-

Table 5. Exergy destructed rate in various components

Component	Exergy destructed (kW)
TCRS	
Compressor	9.906
Evaporator	3.621
Gas Cooler (GC ₁)	3.293
Gas Cooler (GC ₂)	2.65
RHX	4.38
RTV _{TC}	15.28
Total _{TCRS}	39.13
VARs	
Evaporator	0.80
Condenser	0.81
Absorber	2.39
Generator	2.75
SHX	0.36
STV	0.01
RTVVA	0.12
Total _{VARs}	7.219
Net Exergy Destruction	46.35

Table 6. Performance parameters (COP and η_{ex}) comparison with the base TCRS

	TCRS	SEVARs	Combined system	% increase
COP	1.91	0.78	2.38	24.88
η_{ex} (%)	21.33	17.62	23.49	10.14

4.3. Exergy Destruction

Figure 6 presents the exergy destruction in various components of TCRS & SEVARs. It is found that the exergy destruction in SEVAR is maximum in generator followed by absorber and condenser, while the exergy destruction in TCRS is maximum in RTV_{TC} followed by compressor, RHX, evaporator, GC₁ and GC₂ respectively. The exergy destruction of the components implies us to use the components with higher energy efficiency. Therefore to improve the performance of SEVARs, the design of generator & absorber should be focused. In TCRS, the energy can be recovered by replacing the throttling valve with other expansion devices such as expander, ejector, work recovery turbine etc. to further progress the performance of the combined system.

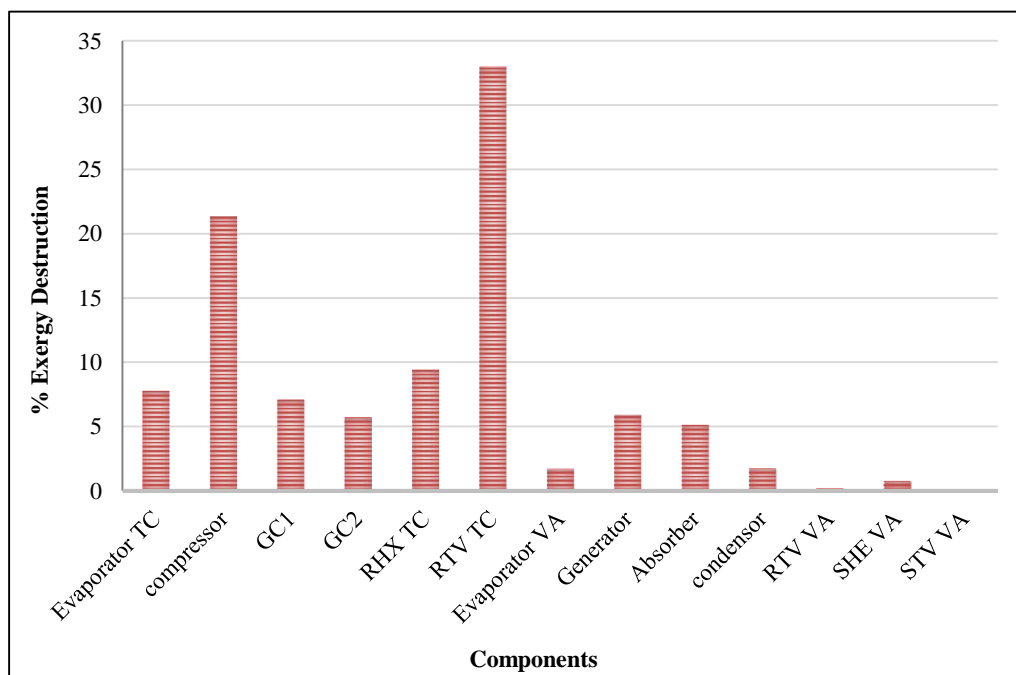


Figure 6. Exergy destructed in various components

4.4. Gas Cooler Pressure

Figure 7 presents the variation of P_{GC} with TCRS evaporation temperature T_{ETC} with different outlet temperature of gas cooler. The P_{GC} is an important parameter in tc- CO_2 compression refrigeration system. The P_{GC} depends upon the exit temperature of gas cooler and the temperature of evaporator [17]. The P_{GC} declines as the evaporator temperature increases, while it increases as the outlet temperature of gas cooler (T_4) increases. The gas cooler pressure is the deciding factor in sizing the components of the transcritical refrigeration system and has an influence on the COP of the system. To maximize the performance parameters of TCRS, the optimum P_{GC} is approximated to be 10 MPa for an evaporator temperature at $-10^\circ C$ and outlet temperature of gas cooler (T_4) being $40^\circ C$.

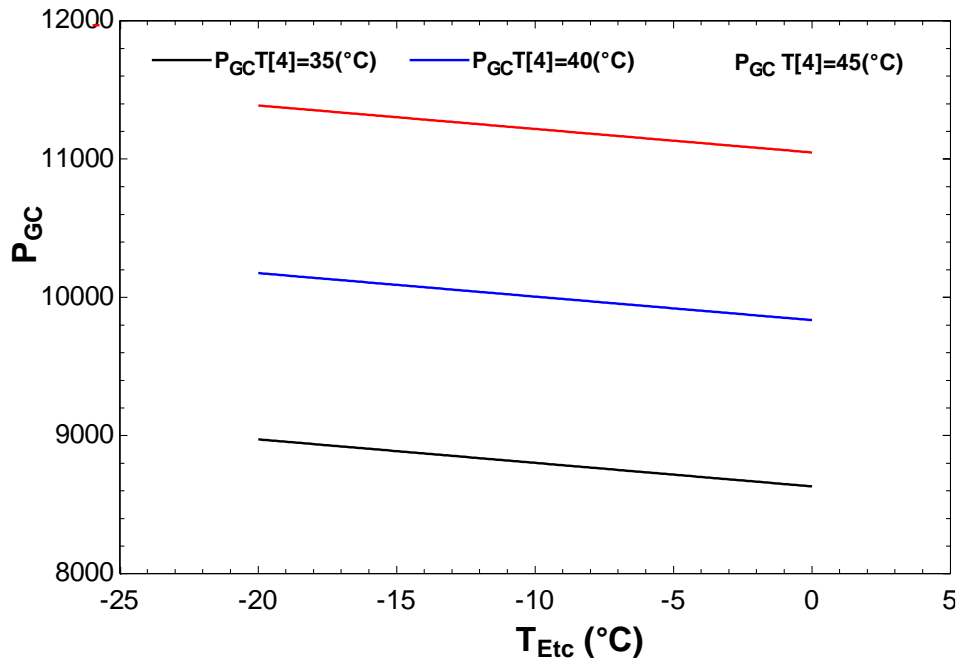


Figure 7. Influence of evaporator temperature of TCRS on P_{GC} at different T_4

4.5. COP vs Evaporator Temperature

Figure 8 presents the trend of COP_{TCRS} and COP_{NET} (combined system) with temperature of evaporator. Both the COP trends increases with the increase in evaporating temperature. This is due to the fact, as the temperature of evaporator increases, the work of compressor decreases and hence the COP. The utilization of waste heat from the gas cooler has increased the cooling capacity of TCRS, also provides additional cooling capacity is observed through SEVARS.

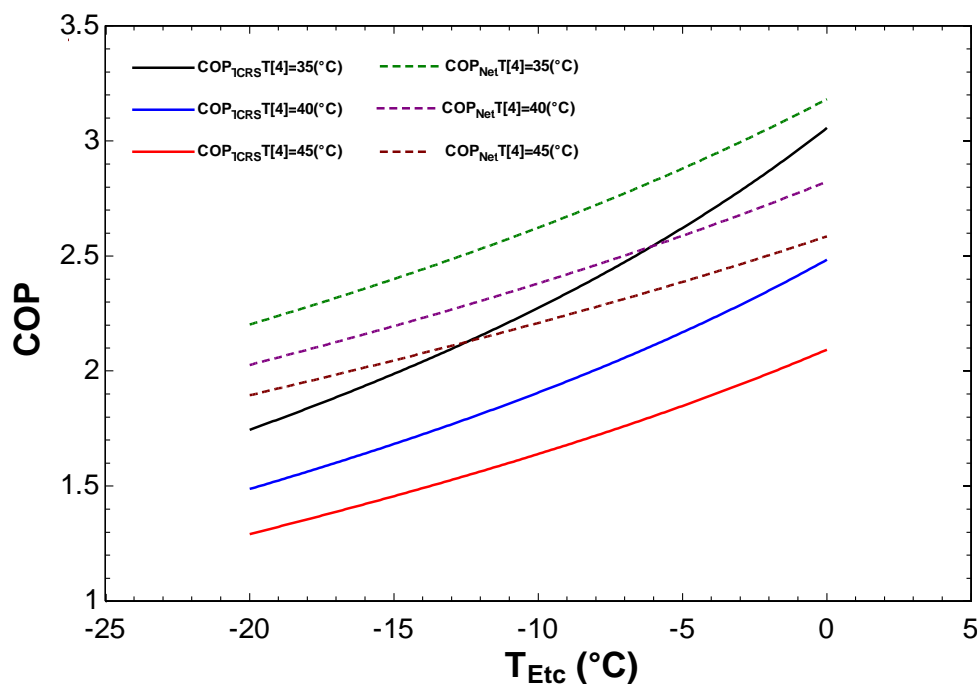


Figure 8. Influence of evaporator temperature of TCRS on COP at different T_4

4.6. Exergetic Efficiency (η_{ex}) vs. Evaporating Temperature

Figure 9 presents the trends of exergetic efficiency (η_{ex}) of TCRS and the combined system with the TCRS evaporating temperature with changed gas cooler outlet temperature. It is observed that the refrigerating temperature has a dominant effect on the exergetic efficiency of the combined system. Both the exergetic efficiencies get the optimum peak and decreases gradually with the increase in evaporating temperature, as the maximum work potential to brought to the system to the environmental conditions decreases as the temperature of evaporator increases and hence the exergetic efficiency.

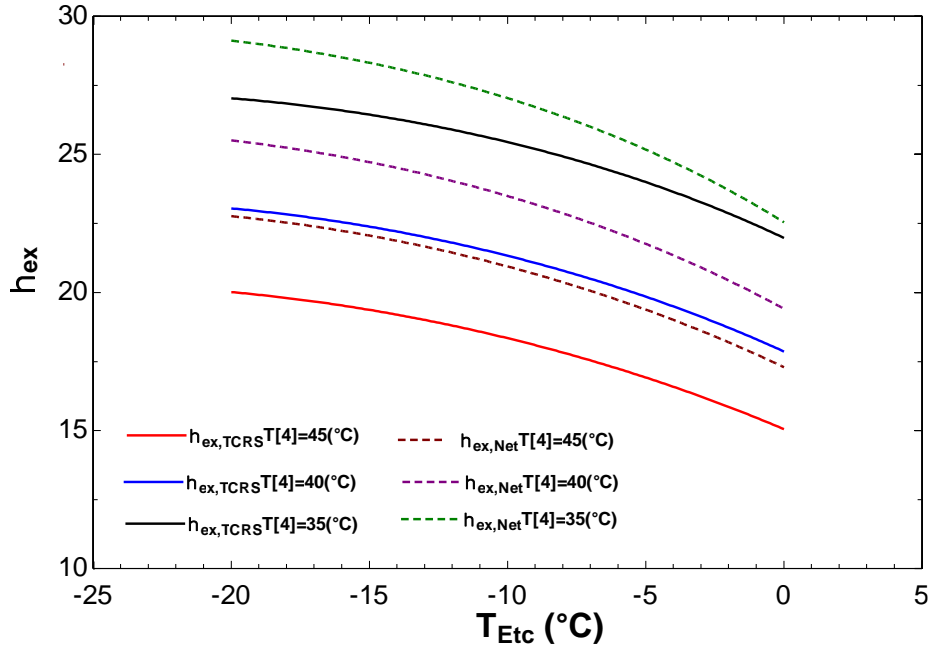


Figure 9. Influence of evaporator temperature of TCRS on (η_{ex}) at different T_4

5. Conclusions

The following conclusions have been drawn from the results:

- Coupling the two cycles increases the COP of the system interestingly. The COP of the combined system increases by 24.88% while the exergetic efficiency is increased by 10.14% over the modified TCRS having RHX_{TC} .
- There is an optimum gas cooler pressure for an evaporator temperature and a gas cooler outlet temperature of T_4 for TCRS. PGC is found to be 10 MPa at an evaporation temperature of -10°C and a T_4 temperature of 40°C .
- The COP of the system increases as the evaporation temperature increases. On the contrary, it decreases with the rise in outlet temperature of the gas cooler.
- The exergetic efficiency shows a peak with the evaporation temperature, which further decreases with the increase in the evaporation temperature. However, it increases with T_4 .
- Efficient compressors and heat exchangers would result in an increase in the performance of the combined system.
- The exergy destructed in RTV_{TC} is considerably high; therefore, replacement of the throttling (expansion) valve by an expander, ejector, and work-recovery turbine will contribute to an increase in the performance of the system.

6. Declarations

6.1. Author Contributions

A.V.: Conceptualization, Writing - Original Draft preparation, Formal analysis, Methodology; S.K.T.: Formal analysis, Writing- Reviewing and Editing, Supervision; S.C.K.: Conceptualization, Reviewing and Editing, Supervision.

6.2. Data Availability Statement

The data presented in this study are available in article.

6.3. Funding and Acknowledgements

The support of Ministry of Education (MOE), and Ministry of New and Renewable Energy (MNRE), Government of India is duly acknowledged.

6.4. Declaration of Competing Interest

The authors declare that they have no known competing financial interests or personal relationships that could have appeared to influence the work reported in this paper.

7. References

- [1] Medical and Chemicals Technical Options Committee. (1987). Montreal protocol on substances that deplete the ozone layer. Washington, DC, US Government Printing Office, 26, 128-136.
- [2] Fartaj, A., Ting, D. S.-K., & Yang, W. W. (2004). Second law analysis of the transcritical CO₂ refrigeration cycle. *Energy Conversion and Management*, 45(13-14), 2269–2281. doi:10.1016/j.enconman.2003.07.001.
- [3] Robinson, D. M., & Groll, E. A. (1998). Efficiencies of transcritical CO₂ cycles with and without an expansion turbine: Efficiency of transcritical CO₂ cycles with and without an expansion turbine. *International Journal of Refrigeration*, 21(7), 577–589. doi:10.1016/s0140-7007(98)00024-3.
- [4] Ma, Y., Liu, Z., & Tian, H. (2013). A review of transcritical carbon dioxide heat pump and refrigeration cycles. *Energy*, 55, 156–172. doi:10.1016/j.energy.2013.03.030.
- [5] Pearson, A. (2005). Carbon dioxide—new uses for an old refrigerant. *International Journal of Refrigeration*, 28(8), 1140–1148. doi:10.1016/j.ijrefrig.2005.09.005.
- [6] Gullo, P., Hafner, A., & Banasiak, K. (2018). Transcritical R744 refrigeration systems for supermarket applications: Current status and future perspectives. *International Journal of Refrigeration*, 93, 269–310. doi:10.1016/j.ijrefrig.2018.07.001.
- [7] Llopis, R., Nebot-Andrés, L., Sánchez, D., Catalán-Gil, J., & Cabello, R. (2018). Subcooling methods for CO₂ refrigeration cycles: A review. *International Journal of Refrigeration*, 93, 85–107. doi:10.1016/j.ijrefrig.2018.06.010.
- [8] Bellos, E., & Tzivanidis, C. (2019). CO₂ Transcritical Refrigeration Cycle with Dedicated Subcooling: Mechanical Compression vs. Absorption Chiller. *Applied Sciences*, 9(8), 1605. doi:10.3390/app9081605.
- [9] Liu, X., Fu, R., Wang, Z., Lin, L., Sun, Z., & Li, X. (2019). Thermodynamic analysis of transcritical CO₂ refrigeration cycle integrated with thermoelectric subcooler and ejector. *Energy Conversion and Management*, 188, 354–365. doi:10.1016/j.enconman.2019.02.088.
- [10] Astrain, D., Merino, A., Catalán, L., Aranguren, P., Araiz, M., Sánchez, D., ... Llopis, R. (2019). Improvements in the cooling capacity and the COP of a transcritical CO₂ refrigeration plant operating with a thermoelectric subcooling system. *Applied Thermal Engineering*, 155, 110–122. doi:10.1016/j.applthermaleng.2019.03.123.
- [11] Mohammadi, S. M. H. (2018). Theoretical investigation on performance improvement of a low-temperature transcritical carbon dioxide compression refrigeration system by means of an absorption chiller after-cooler. *Applied Thermal Engineering*, 138, 264–279. doi:10.1016/j.applthermaleng.2018.04.006.
- [12] Bellos, E., & Tzivanidis, C. (2019). Enhancing the performance of a CO₂ refrigeration system with the use of an absorption chiller. *International Journal of Refrigeration*, 108, 37–52. doi:10.1016/j.ijrefrig.2019.09.009.
- [13] Neksa, P. (2002). CO₂ heat pump systems. *International Journal of Refrigeration*, 25(4), 421–427. doi:10.1016/s0140-7007(01)00033-0.
- [14] Lo Basso, G., de Santoli, L., Paiolo, R., & Losi, C. (2021). The potential role of trans-critical CO₂ heat pumps within a solar cooling system for building services: The hybridised system energy analysis by a dynamic simulation model. *Renewable Energy*, 164, 472–490. doi:10.1016/j.renene.2020.09.098.
- [15] Liu, Z., Xie, N., & Yang, S. (2020). Thermodynamic and parametric analysis of a coupled LiBr/H₂O absorption chiller/Kalina cycle for cascade utilization of low-grade waste heat. *Energy Conversion and Management*, 205, 112370. doi:10.1016/j.enconman.2019.112370.
- [16] Dincer, I., & Rosen, M. A. (2012). *Exergy: energy, environment and sustainable development*. Elsevier Science, Netherlands. doi:10.1016/C2010-0-68369-6.
- [17] Sarkar, J., Bhattacharyya, S., & Gopal, M. R. (2004). Optimization of a transcritical CO₂ heat pump cycle for simultaneous cooling and heating applications. *International Journal of Refrigeration*, 27(8), 830–838. doi:10.1016/j.ijrefrig.2004.03.006.
- [18] Pérez-García, V., Rodríguez-Muñoz, J. L., Ramírez-Minguela, J. J., Belman-Flores, J. M., & Méndez-Díaz, S. (2016). Comparative analysis of energy improvements in single transcritical cycle in refrigeration mode. *Applied Thermal Engineering*, 99, 866–872. doi:10.1016/j.applthermaleng.2016.01.092.

- [19] Arora, A., Singh, N. K., Monga, S., & Kumar, O. (2011). Energy and exergy analysis of a combined transcritical CO₂ compression refrigeration and single effect H₂O-LiBr vapour absorption system. *International Journal of Exergy*, 9(4), 453. doi:10.1504/ijex.2011.043916.
- [20] Arora, A., & Kaushik, S. C. (2009). Theoretical analysis of LiBr/H₂O absorption refrigeration systems. *International Journal of Energy Research*, 33(15), 1321–1340. doi:10.1002/er.1542.
- [21] Verma A, Arora A, & Mishra R S (2016). Energy Analysis and Optimization of Flat Pate Collector Area of a Solar Driven Water-Lithium Bromide Half Effect Vapour Absorption Refrigeration System for a given Cooling Load, *Proceedings of The International Conference on Recent Advances In Mechanical Engineering*, DTU Delhi, India, 521-528.
- [22] Herold, K. E., Radermacher, R., & Klein, S. A. (2016). *Absorption chillers and heat pumps*. CRC Press, Florida, United States.
- [23] Pátek, J., & Klomfar, J. (2006). A computationally effective formulation of the thermodynamic properties of LiBr–H₂O solutions from 273 to 500K over full composition range. *International Journal of Refrigeration*, 29(4), 566–578. doi:10.1016/j.ijrefrig.2005.10.007.
- [24] Bejan, A., Tsatsaronis, G., and Moran, M. J. (1995). *Thermal design and optimization*. John Wiley & Sons, New York, United States.